Autoionizing states of He: Projectile-velocity-dependent lifetime

S. Otranto,[1,2] C. R. Garibotti,[1] F. D. Colavecchia,[1] and G. Gasaneo[2]
[1]CONICET and Centro Atómico Bariloche, 8400 San Carlos de Bariloche, Río Negro, Argentina
[2]CONICET and Departamento de Física, Universidad Nacional del Sur, Av. Alem 1253, 8000 Bahía Blanca, Buenos Aires, Argentina

(Received 13 July 2000; published 18 January 2001)

In this work, we study the dependence of the lifetime (τ) of an autoionizing state with the velocity (v_P) of an ionic projectile of charge Z. We use a C2 model to represent the final state of the autoionized electron in the continuum of two centers. Explicit calculations for the helium autoionizing states $2s^2(^1S)$, $2p^2(^1D)$, and $2s2p(^1P)$ are analyzed. We evaluate the decay law for the metastable initial state and find that τ increases as the projectile becomes faster and converges to the photoionization lifetime for high impact energies. A scaling law for τ is obtained in terms of the Sommerfeld parameter (Z/v_P). Finally, we evaluate the transition probability for the autoionized electron and show that the mean half-width of the focusing peak decreases as v_P increases.

DOI: 10.1103/PhysRevA.63.022713 PACS number(s): 34.50.Fa

I. INTRODUCTION

In the past few years, the theoretical description of the autoionization process has been improved by several semiclassical and quantum models [1–6]. The atomic autoionization process by ion impact consists of a two-step process. The first one is the excitation of an atom by a heavy projectile. The second is the decay of the excited state and the emission of an electron to the continuum. The first model proposed to describe this effect was presented by Barker and Berry [7], based on phenomenological grounds. In their work, they studied the SDCS as a function of the autoionized electron energy. They observed that as the projectile energies are lowered, the autoionization peak shapes become wider and more asymmetric. This could be linked to the fact that a wider peak shape is related with a shorter lifetime of the excited state. The first quantum-mechanical model was developed by Devdariani *et al.* [1] and neglects the interaction between the autoionized electron and the projectile, this interaction being represented by a plane wave. This approximation implies that the projectile modifies the energy but has no influence on the trajectory of the emitted electron. This model is not consistent since, due to its infinite range, the electron-projectile Coulomb interaction does not vanish at large distances. The eikonal model proposed by Morgenstern *et al.* [2] preserves a logarithmic distortion to represent the electron-projectile interaction in an asymptotic form. Although it introduces more information about the postcollisional interaction than the previous model, the angular distribution predicted by this model was incorrect for small angles in momentum space of the autoionized electron. Barrachina and Macek have shown that their continuum distored-wave (CDW) model [3], representing the electron-projectile interaction with a Kummer function, contains previous models as particular cases in different regions of the velocity space. Furthermore, this model successfully predicted the existence of a sharp enhancement in the intensity profile for electrons ejected at zero angle. The electrons emitted at small angles are in the continuum of two centers and become focused by the field of the projectile. That is to say, this model predicts that the postcollisional interaction of the projectile does affect the trajectories of the autoionized electrons. This behavior, known as *Coulomb focusing*, was observed experimentally by Swenson *et al.* in 1989 [8]. Other authors studied the Stark effect for the autoionizing states of helium [4,5]. In their works, they explore the fact that a low-energy projectile (below 10 keV for He^+-He) could excite an atom not to a definite state but to a mixture of excited states.

The transition amplitude for the autoionization process can be written as [9]

$$b(\alpha,t)=-i\int_0^t dt'\, e^{i(E-E_0)t'-\int_0^{t'}dt''[\Gamma(v_P,t'')/2]}\,t'^{\,i(Z/v_p)}\times\left\langle \alpha\left|\frac{1}{r_{12}}\right|\varphi_i\right\rangle, \tag{1}$$

where

$$\frac{\Gamma(v_P,t)}{2}=\pi\int d\Omega\left[v\left|\left\langle \alpha\left|\frac{1}{r_{12}}\right|\varphi_i\right\rangle\right|^2\right]_{v=\sqrt{2E_0}}. \tag{2}$$

Here E_0 represents the resonant energy, Z the projectile charge, v_P the projectile velocity, $1/r_{12}$ represents the interelectronic repulsion that is considered as perturbation, φ_i is the autoionizing state, and α is the final state consisting of an electron in the continuum and the other one in a bound state. The solid angle element of the integral is $d\Omega=\sin\theta d\theta d\phi$, where θ is the angle between the projectile velocity vector $\mathbf{v}_P$ and the autoionized electron velocity vector $\mathbf{v}$. The photoionization values for Γ are used in the CDW model. The Γ is related to the inverse of the lifetime of the autoionizing state and is assumed independent of the projectile. However, the emitted electron is in a continuum state of two ionic centers and, therefore, the lifetime of the discrete initial state must depend on the projectile velocity. That is not taken into account in former models. In this paper, we work out the relation between two center functions and excited-state lifetimes. The autoionizing initial state could be represented by products of hydrogeniclike functions [10] with effective charges.

The hydrogenic one-electron wave functions are a good approximation at intermediate distances from the nucleus and these functions are assumed to be orthogonal due to the small difference between the self-consistent fields for the initial and final configurations. The final-state wave function depends on the approximation taken for the kinetic-energy operator. The C2 function $|\alpha_t\rangle|\alpha_p\rangle$, i.e., a product of continuum wave functions centered in the target and projectile, is the solution corresponding to an uncorrelated problem. That is to say, it considers the final state of an electron in two centers as the product of two wave functions, each one being a solution of a two-body Coulomb problem. More elaborate wave functions can be proposed as expansions in terms of Kummer functions to represent the electron in the continuum of both target and projectile. For these expansions, the C2 function becomes the zero-order term as has been proved by Gasaneo *et al.* [11]. Their Φ_2 model leads to a two-variable confluent hypergeometric function, which gives a kinematically correlated picture of an electron in the continuum of two centers. Such functions seem to be a good way to introduce the information contained in the nondiagonal kinetic energy, usually neglected. In this work, using an independent-particle model, we consider the autoionizing processes for He^+ colliding with He in the intermediate metastable states $2s^2(^1S)$,$2p^2(^1D)$,$2s2p(^1P)$.

To represent the final continuum state of the ejected electron, we use an uncorrelated C2 model. In Sec. II, we summarize the main calculations that have been performed to obtain the time integral of Γ. The main contributions to the time-dependent transition amplitude are shown for the three autoionizing states studied. In Sec. III, some conclusions and outlooks are drawn. Possible implications of the introduction of a correlated wave function for the final state of the autoionized electron are also mentioned. Atomic units are used unless otherwise stated.

II. THE C2 MODEL

The important advance given by the C2 model consists in the better description of the angular distribution of the autoionized electrons, as we have already pointed out in the Introduction. Our main objective is to investigate the possible dependence of the lifetime of an excited state with the projectile velocity. For that reason, in this section we calculate the transition matrices needed to obtain an expression for the time integral of Γ that appears in Eq. (1). From Eq. (2),

$$\frac{\Gamma(v_P,t)}{2}=\pi\int d\Omega\,\sqrt{2E_0}|A_0|^2[|\alpha_p|^2]_{v=\sqrt{2E_0}},$$
$$|A_0|^2=\left[\left|\left\langle \alpha_t\left|\frac{1}{r_{12}}\right|\varphi_i\right\rangle\right|^2\right]_{v=\sqrt{2E_0}}, \tag{3}$$

where, in an impact parameter approximation [3],

$$\alpha_p=e^{(\pi Z/2v')}\Gamma\left(1+\frac{iZ}{v'}\right)\,{}_1F_1\left[-i\frac{Z}{v'},1,-i(v_Pv'-\mathbf{v}_P\cdot\mathbf{v}')t\right] \tag{4}$$

and $\mathbf{v}'$ is the velocity of the electron relative to the projectile.

In Eq. (4), a peaking approximation has been performed since the integrand of the matrix element $\langle\alpha_t|1/r_{12}|\varphi_i\rangle$ is strongly confined to the vicinity of the target nucleus [3].

For the three excited states, Eq. (3) should reduce to the known photoionization values Γ_{ph} when one sets $Z=0$. To calculate the transition matrix elements, we propose the wave functions

$$\varphi_{n_1,n_2}(\mathbf{r}_1,\mathbf{r}_2)=\phi_{n_1}(\lambda,\mathbf{r}_1)\phi_{n_2}(\lambda,\mathbf{r}_2), \tag{5}$$

where $\phi_{n_i}(\lambda,\mathbf{r}_j)$ is a hydrogenic wave function with effective charge λ. For the $2s2p(^1P)$ state, we use the wave function

$$\varphi_{2s,2p}(\mathbf{r}_1,\mathbf{r}_2)=\frac{1}{\sqrt{2}}\{\phi_{2s}(\lambda,\mathbf{r}_1)\phi_{2p}(\beta,\mathbf{r}_2)+\phi_{2s}(\lambda,\mathbf{r}_2)\phi_{2p}(\beta,\mathbf{r}_1)\}. \tag{6}$$

Although more elaborate wave functions could be used in these calculations, they notably simplify the analytical work to be performed giving the main features of the process. Following Kostroun *et al.* [10], we perform the analytical calculation of $\langle\alpha_t|1/r_{12}|\varphi_i\rangle$, writing $\langle\alpha_t|$ as an expansion in partial waves. This is just the two-body Coulomb wave function expanded in partial waves [12]. Then, in order to calculate the matrix elements, we must perform an integral in radial coordinates r_1 and r_2 and an angular integral involving θ_1, ϕ_1, θ_2, and ϕ_2. The angular integral could be written in terms of the Clebsch-Gordan coefficients, which restrict the possible values for the quantum numbers.

The integrals in Eq. (3) are performed numerically. For the three excited states, we assume that the effective charge of the target seen by the electron once ionized is $Z_T^*=1$ and choose the λ value that yields the experimental Γ_{ph} when the projectile charge is turned off $(Z=0)$. As a result, we obtain $\lambda=1.5055$ for the $2s^2(^1S)$ state, $\lambda=1.3425$ for the $2p^2(^1D)$ states, and $\lambda=1.565$ and $\beta=1$ for the $2s2p(^1P)$ state.

The values used for E_0 are 1.224, 1.297, and 1.307 a.u. and for Γ_{ph} they are 0.005 07, 0.002 65, and 0.0014 a.u., each one corresponding, respectively, to $2s^2(^1S)$, $2p^2(^1D)$, and $2s2p(^1P)$ [5].

Now we consider the decay law for the metastable atomic states:

$$b_i(v_P,t)=\exp\left(-\int_0^t dt'\frac{\Gamma(v_P,t')}{2}\right). \tag{7}$$

The value $|b_i(v_P,t)|^2$ represents the probability that the electron stays in the excited state at time *t*. For $t=0$, $b_i(0)=1$ and the system is in the corresponding excited state. In Fig. 1, we have plotted $|b_i(v_P,t)|^2$ as a function of time. As can be seen when the autoionized electron-projectile interaction is taken into account, the continuum states are populated more rapidly than in the photoionization case. That is to say, the time τ that $|b_i(v_P,t)|^2$ takes to decay to the value e^{-1} is shorter when the autoionized electron-projectile interaction is considered. When the projectile velocity is incremented,

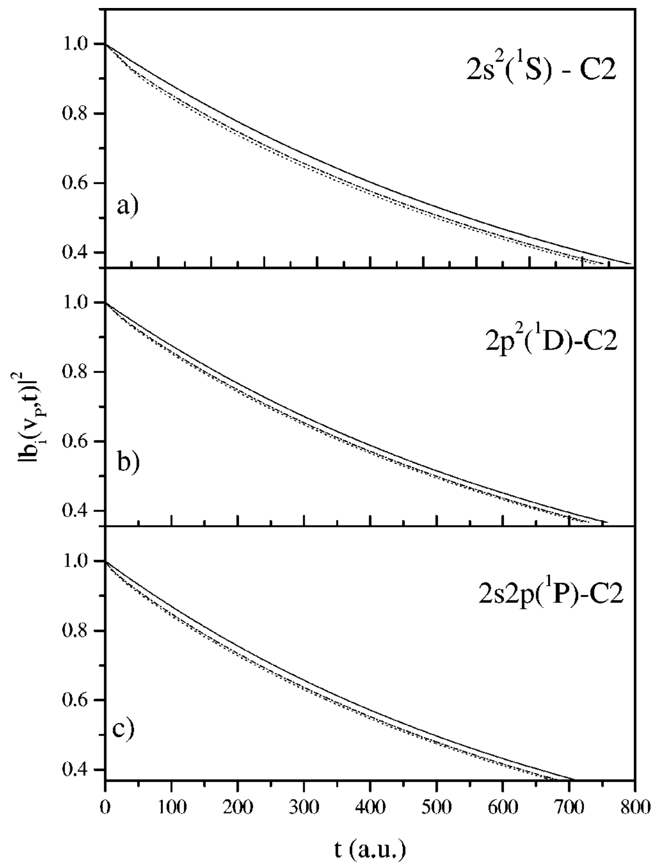

FIG. 1. $|b_i(v_P,t)|^2$ as function of time for the three autoionizing states studied. (a) $2s^2(^1S)$; (b) $2p^2(^1D)$; (c) $2s2p(^1P)$. In all cases: dot-line, for $E_{\rm projectile}=5$ keV; dash-dot-line, for $E_{\rm projectile}=15$ keV. Solid line, $\exp(-\Gamma_{\rm ph}t)$. Here $Z=1$.

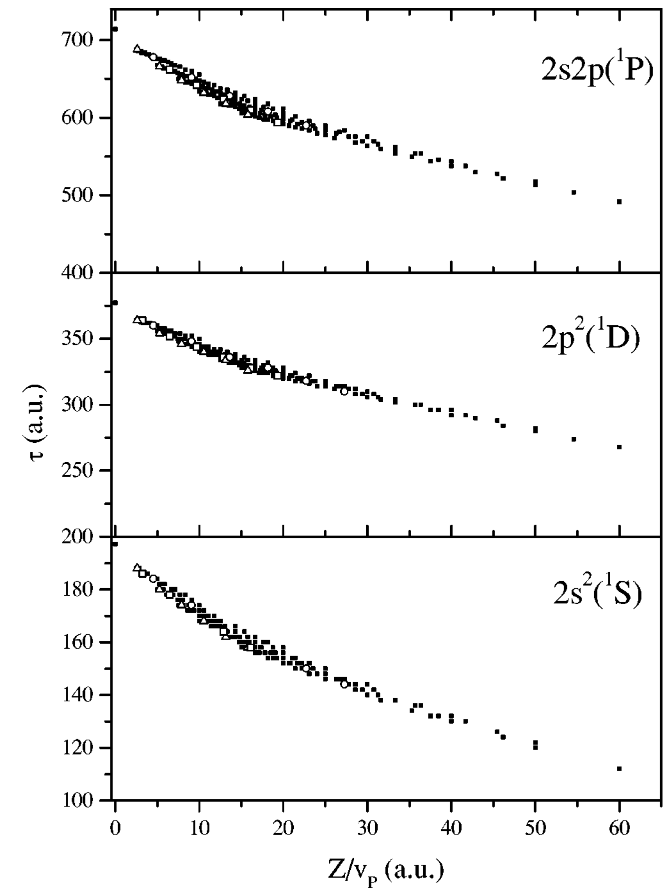

FIG. 2. Time τ as a function of Z/v_P for the three autoionizing states. Three He^+ projectile incident energies are identified: circle, 5 keV; square, 10 keV; up-triangle, 15 keV.

the collision time is shorter and the results become closer to the photoionization ones. In the limit $v_P\to\infty$, the photoionization curves are recovered. In Table I, the τ values are given for the three autoionizing states and are compared with the photoionization ones. In Fig. 2, we plot τ as a function of the Sommerfeld parameter Z/v_P for the three autoionizing states studied. The v_P values are varied between 0.1 a.u. (1 keV for He^+) and 0.4 a.u. (16 keV for He^+), and we consider Z an integer number between 0 and 6. For $Z/v_P=0$, we recover the photoionization values $\tau_{\rm ph}=\Gamma_{\rm ph}^{-1}$. This case corresponds to $Z_p=0$ or $v_P\to\infty$, and represents null interaction between the projectile and the autoionized electron. As the quotient value increases, the τ values decrease as shown, giving a clear picture of how slow projectiles modify the lifetime of the excited states.

TABLE I. Mean lifetime of initial states, i.e., time values to obtain $|b_i(v_P,t)|^2=e^{-1}$.

		τ		
v_P (a.u.)	E (keV)	$2s^2(^1S)$	$2p^2(^1D)$	$2s2p(^1P)$
0.220	5	183	360	676
0.316	10	186	363	682
0.387	15	187	364	684
Photoionization		197.23	377.35	714.285

A scaling law of τ with Z/v_P can be obtained with a nonlinear fitting procedure. We proposed

$$\tau=a\left[\frac{Zp}{v_P}\right]^b+c \tag{8}$$

with fitting parameters a,b. The c value is taken equal to $\tau_{\rm ph}$ such that for $Z/v_P=0$ one recovers $\tau=\tau_{\rm ph}$. In Table II, the a, b, and c values are given for the three autoionizing states studied, and they give the best fitting to τ. The errors associated with the fitting parameters in Eq. (8) are of about $\pm 2\%$ for a and $\pm 1\%$ for b.

The autoionization probability is obtained by a further numerical integration of Eq. (1). In Fig. 3, we show $|b(v_P,\alpha)|^2$ as a function of the autoionizing electron velocity at 0° for the $2s^2(^1S)$ state. There, we plot the focusing

TABLE II. Fitting parameters from Eq. (8), obtained to get the best fitting of τ as a function of Z/v_P.

Fit. Par.	$2s^2(^1S)$	$2p^2(^1D)$	$2s2p(^1P)$
a	−5.623	−7.283	−16.379
b	0.673	0.664	0.644
c	197.230	377.350	714.285

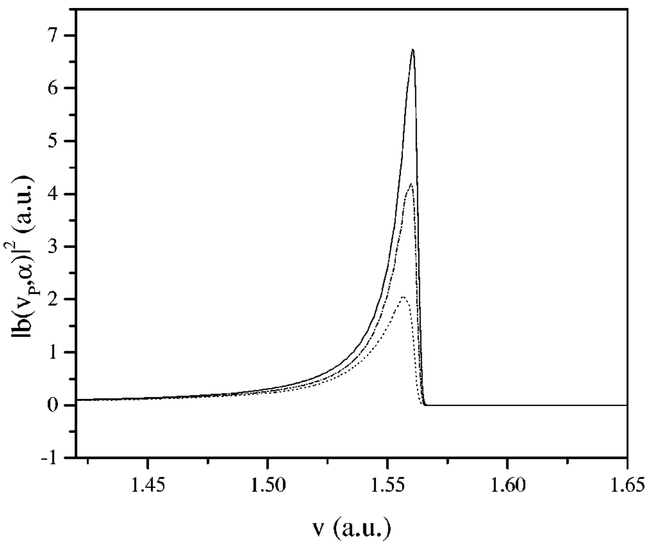

FIG. 3. Autoinization probability $|b(v_P,\alpha)|^2$ as a function of v for the $2s^2(^1S)$ state. Lines as in Fig. 1.

peak at three different collision energies. As can be seen, for lower energies the intensity of the peak decreases and the full width at half maximum of the peak increases. However, the main effect is not produced by the dependence of Γ with v_P. To analyze this situation, we evaluate the transition amplitude for the autoionization process by noting that it is possible a linear fit for long times:

$$\int_0^t dt' \Gamma(v_P,t') = A(v_P) + \Gamma_{\mathrm{ph}} t. \tag{9}$$

This can be easily included in Eq. (1), incorporating the projectile velocity dependence in A. Some values obtained for A from Eq. (9) are listed in Table III for the three autoionized states studied.

The transition amplitude obtained from Eq. (1) considering Eq. (9) remains:

$$b(v_P,\alpha) = -ie^{-A(v_P)/2}\int_0^\infty dt' \times e^{i(E-E_0)t' - (\Gamma_{\mathrm{ph}}/2)t'} t'^{\,i(Z/v_p)} \left\langle \alpha \left| \frac{1}{r_{12}} \right| \varphi_i \right\rangle. \tag{10}$$

TABLE III. Values for $A(v_P)$ as given by Eq. (9) as a function of the projectile velocity for the three helium autoionizing states studied.

			$A(v_P)$	
v_P (a.u.)	E (keV)	$2s^2(^1S)$	$2p^2(^1D)$	$2s2p(^1P)$
0.22	5	0.121	0.085	0.084
0.27	7.5	0.105	0.074	0.073
0.32	10	0.096	0.069	0.067
0.38	15	0.087	0.063	0.061
0.54	30	0.081	0.058	0.056

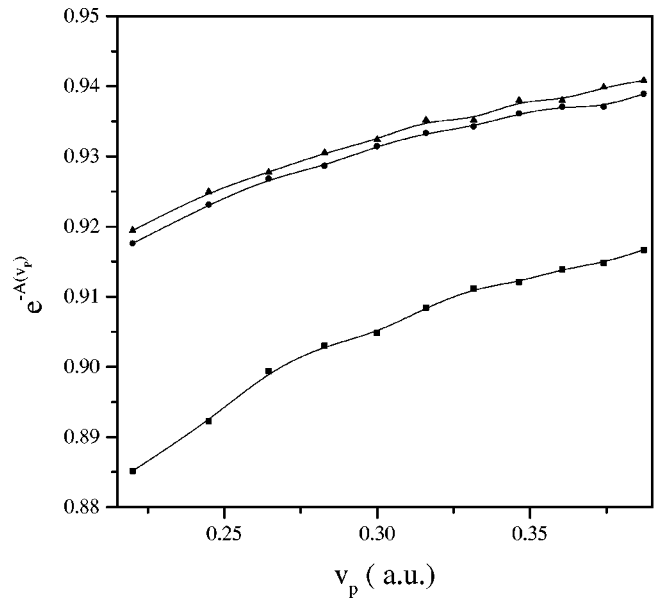

FIG. 4. Factor $e^{-A(v_P)}$ as a function of the projectile velocity v_P, corresponding to the range of projectile energies (5 keV–15 keV) for the three autoionizing states studied: square, $2s^2(^1S)$; circle, $2p^2(^1D)$; triangle, $2s2p(^1P)$.

This is equivalent to the results of previous models, except by a multiplying factor $e^{-A(v_P)}$, which modulates the intensity profiles for different projectile velocities. Figure 4 shows the dependence of $e^{-A(v_P)}$ with the projectile velocity. The range of projectile energies studied was between 5 keV and 15 keV. As can be seen, this quantity varies smoothly with the projectile velocity for the three excited states and $A \rightarrow 0$ when $v_P \rightarrow \infty$. The state $2s^2(^1S)$ seems to be the more affected one by the action of the projectile. This could be due to the fact that we carry on a zero impact parameter approximation and the $2s^2(^1S)$ state is located closer to the target nucleus than the other states.

Now we can consider again Fig. 3. The v_P dependence of the mean life of the initial metastable state gives a small multiplicative correction to the curves, as observed from Fig. 4. The final-state three-body function used in the evaluation of the interaction matrix determines the main dependence of the peak with v_P.

We analyze the angular distributions by defining, following Cordrey and Macek [5],

$$w(v_P,\Omega) = \int_0^\infty b^*(v_P,\alpha) b(v_P,\alpha) dE, \tag{11}$$

which is proportional to the cross section $d\sigma/d\Omega$ and $E = v^2/2$. We extend the lower integration limit to $-\infty$, proving that for $E<0$, $b(\alpha)=0$. Performing a peaking approximation $v=v_a=\sqrt{2E_0}$, only a common factor exp($iEt - iEt'$) remains under the energy integral. With

$$\int_{-\infty}^{\infty} e^{iE(t-t')} dE = 2\pi\delta(t-t'),$$

Eq. (11) remains,

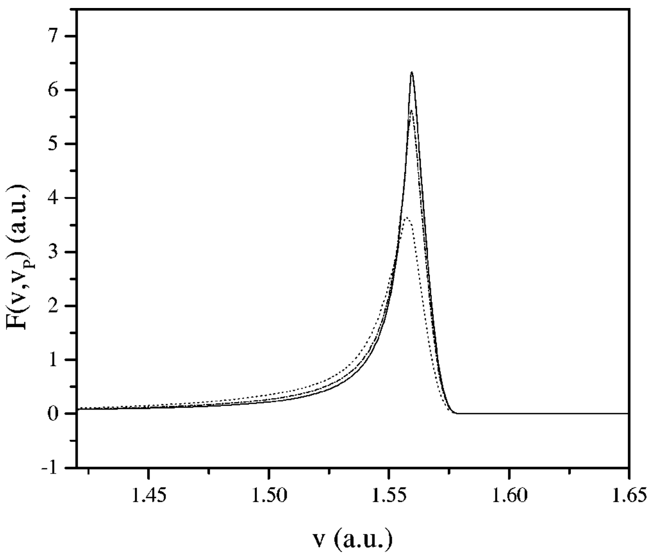

FIG. 5. $F(v,v_P)$ as a function of v. The He^+ projectile incident energies are solid line, 15 keV; dash-dot-line, 10 keV; dot-line, 5 keV.

$$w(v_P,\Omega)=2\pi|A_0|^2\left|\Gamma\left(1-\frac{Z}{v_a'}\right)\right|^2 e^{\pi(Z/v_a')}\int_0^\infty e^{-\int_0^t\Gamma(v_P,t')dt'}\times {}_1F_1\left(i\frac{Z}{v_a'},1,i\,d_a t\right){}_1F_1\left(-i\frac{Z}{v_a'},1,-i\,d_a t\right)dt, \quad (12)$$

where $v_a'=[v_a^2+v_P^2-2v_Pv_a\cos(\theta)]^{1/2}$ and $d_a=v_Pv_a'-\mathbf{v}_P\cdot\mathbf{v}_a'$. With Eq. (11), we can write Eq. (12) in terms of the Gauss hypergeometric function ${}_2F_1(a,b,c,z)$ as follows [13]:

$$w(v_P,\Omega)=2\pi\frac{|A_0|^2}{\Gamma_{\rm ph}}\frac{\pi Z}{v_a'\sinh(\pi Z/v_a')}\times e^{-A(v_P)}e^{(Z/v_a')[\pi-2\arctan(d_a/\Gamma_{\rm ph})]}\times {}_2F_1\left(i\frac{Z}{v_a'},-i\frac{Z}{v_a'},1,\frac{d_a^2}{d_a^2+\Gamma_{\rm ph}^2}\right). \quad (13)$$

Other than by the exponential factor, this expression is identical to that given by former models. The correction to the shape of the angular distribution is independent of the projectile velocity.

The electron velocity distribution is determined by

$$F(v,v_P)=\int d\Omega|b(v_P,\alpha)|^2, \quad (14)$$

where $d\Omega=2\pi\sin\theta d\theta$. This quantity is proportional to the SDCS in energy. In Fig. 5, we show $F(v,v_P)$ as a function of the autoionized electron velocity. As can be seen, for lower energies the profile of the peak becomes more asymmetric and wider, in agreement with the observations of Barker and Berry.

III. CONCLUSIONS AND OUTLOOK

In this work, we have studied the autoionization of He by ion impact. We have focused our attention on the influence of a He^+ projectile in the properties of the autoionizing states $2s^2(^1S)$, $2p^2(^1D)$, and $2s2p(^1P)$. We make use of a CDW model, where the final state is described by a two-center Coulomb wave function. The autoionizing states of two bound electrons were modeled by a simple symmetrized hydrogenic wave function with effective charges. They have been selected to give the correct $\Gamma_{\rm ph}$ value when the projectile charge is turned off.

We have found that the lifetime of the states is modified by the projectile leaving the collision region. The lifetime decreases when the velocity of the projectile decreases. Furthermore, when the strength of the electron-projectile interaction increases, i.e., Z_p increases, the lifetime also decreases. This fact can be easily understood: the projectile pulls the electron into the continuum more quickly (in a faster way) when the collision time is larger, that is to say, when the velocity v_p is small. The same effect can be obtained by a projectile with a higher charge. A suitable way to represent the combination of these two effects is to plot the lifetime of each state against the Sommerfeld parameter Z_p/v_p. We have found that the lifetimes follow a universal power law, $\tau\propto(Z_p/v_p)^b$, with this Sommerfeld parameter. This scaling is useful to predict the behavior of autoionizing states in more general situations that are frequently hard to obtain experimentally. The limiting cases $Z_p\rightarrow 0$ and/or $v_p\rightarrow\infty$ are also correctly described by our model. We note that our results agree with the lower lifetime values proposed by Morgenstern *et al.* from a fitting procedure using the lifetimes of the autoionizing states as fitting parameters [14]. We have also found that, for long times, an exponential factor modulates the transition amplitude of the collision. This factor has a smooth variation with the projectile energy. This could be important when taking into account the interference between different autoionizing states and with direct ionization, for comparison with experimental DDCS. We would like to point out that these results become more relevant for projectiles of very low energy where the Stark effect should be considered. Their inclusion in a model such as the one developed by Miraglia and Macek [4] or Cordrey and Macek [5] as cited above could be directly performed.

We have obtained the transition amplitudes by numerical integration for the $2s^2(^1S)$ state. We have shown that for lower energies the profile of the focusing peak becomes lower and wider, in agreement with the results of Barker and Berry [7].

Finally, we should note that the use of more sophisticated initial states (that keep the correct $\Gamma_{\rm ph}$ values when the projectile charge is set to zero) and/or the introduction of a correlated two-center wave function to represent the autoionized electron could give even shorter lifetimes than the ones obtained in this work [14].

ACKNOWLEDGMENTS

We would like to thank R. O. Barrachina and J. E. Miraglia for helpful discussions. This work has been supported by the Science and Technology Investigation Project, Grant No. 99-0306249.

[1] A. Z. Devdariani, X. Ostrovskii, and Yu. N. Sebayakin, Zh. Éksp. Teor. Fiz. **73**, 412 (1977) [Sov. Phys. JETP **46**, 215 (1977)].
[2] P. van der Straten and R. Morgenstern, J. Phys. B **18**, 1361 (1986).
[3] R. O. Barrachina and J. H. Macek, J. Phys. B **22**, 2151 (1989).
[4] J. E. Miraglia and J. Macek, Phys. Rev. A **42**, 3971 (1990).
[5] I. L. Cordrey and J. Macek, Phys. Rev. A **48**, 1264 (1993).
[6] Sh. D. Kunikeev and V. S. Senashenko, Zh. Éksp. Teor. Fiz. **109**, 1561 (1996) [JETP **82**, 839 (1996)].
[7] R. P. Barker and H. W. Berry, Phys. Rev. **151**, 14 (1966).
[8] J. K. Swenson, C. C. Havener, N. Stolterfoht, K. Sommer, and F. W. Meyer, Phys. Rev. Lett. **63**, 35 (1989).
[9] C. Cohen-Tannoudji, B. Diu, and F. Laloë, *Quantum Mechanics, Vol. II* (John Wiley & Sons, New York, 1977).
[10] V. O. Kostroun, M. H. Chen, and B. Crasemann, Phys. Rev. A **3**, 533 (1971).
[11] G. Gasaneo, F. D. Colavecchia, C. R. Garibotti, J. E. Miraglia, and P. Macri, Phys. Rev. A **55**, 2809 (1997).
[12] L. I. Schiff, *Quantum Mechanics* (McGraw-Hill Book Company, New York, 1968).
[13] M. Abramowitz and I. A. Stegun, *Handbook of Mathematical Functions* (Dover Publications, Inc., New York, 1964).
[14] R. Morgenstern, A. Niehaus, and U. Thielmann, J. Phys. B **10**, 1039 (1977).